Supplementary Materials

Pyroelectric Field Drived Photocatalysis by $ZnFe_2O_4/NaNbO_3$ Heterojunction for Dye Degradation through Integration of Solar and Thermal Energy

Di Zhou[1,§], Xiaoju Zhou[2,§], Zhenglong Hu[2,*], Lili Zheng[1], Yu Tian[1], Yafang Tu[1], Chunbo Hua[2], Li Xue[2], Juan Xiong[3,*]

[1.] School of Optoelectronic Materials and Technology, Jianghan University, Wuhan 430056, P. R. China

[2.] School of electronic and Information Engineering, Key Laboratory of Optoelectronic Sensing and Intelligent Control, Hubei University of Science and Technology, Xianning 437100, P. R. China

[3.] Hubei Key Laboratory of Micro-nanoelectronic Materials and Devices, School of Microelectronics, Hubei University, Wuhan 430062, P. R. China

*Corresponding Authors: E-mail: huzhenglong@hbust.edu.cn (Zhenglong. Hu); E-mail: juanxiong@hubu.edu.cn (Juan. Xiong)

§ These authors contributed equally to this work.

Contents

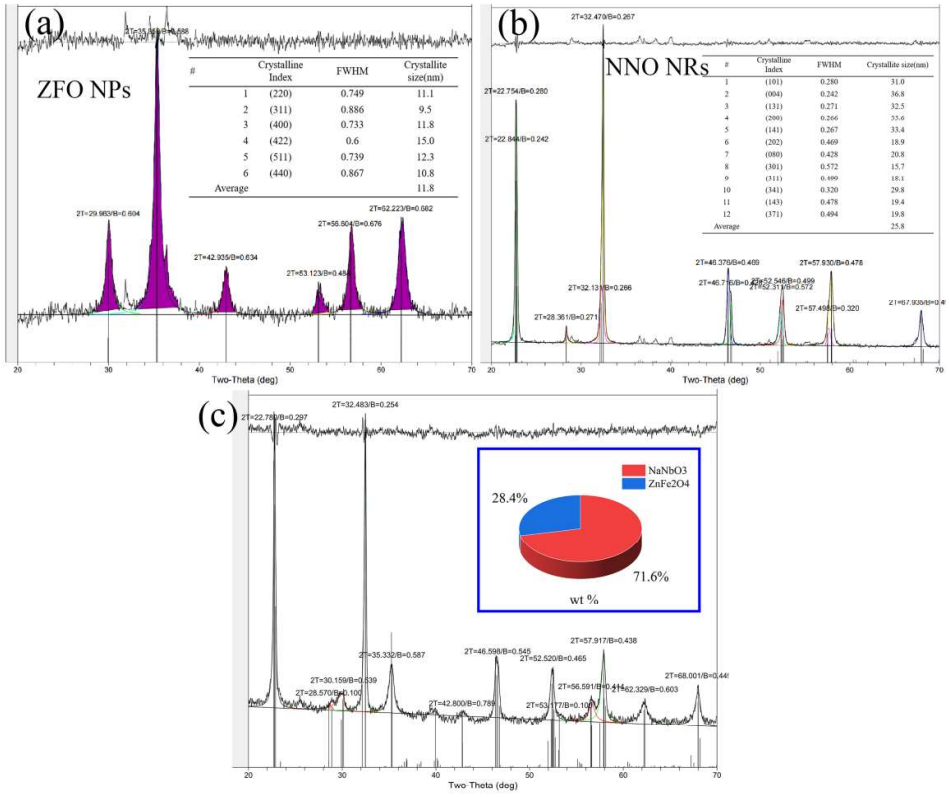

Figure S1. XRD data analysis using the 'MDI Jade' program: the FWHM of the primary diffractions and the grain sizes of (a) ZFO and (b) NNO NRs, (c) the mass percentage content of the two phases (ZFO and NNO) in the ZFO/NNO NRs samples.

The XRD patterns of the NNO NRs and ZFO samples were analysed by using the 'MDI Jade' program (version 6.5, MDI Materials Data Inc., USA). The results of the diffracted crystal planes, FWHM, and their corresponding grain sizes were shown in Figure S1(a) and Figure S1(b). The average grain sizes of the ZFO and NNO were calculated to be approximately 11.8 and 25.8 nm, respectively. It can be seen that a larger FWHM corresponds to a smaller grain size, which is in accordance with Scheller's formula as follows.

$$D = \frac{K\lambda}{\beta \cos\theta}$$

Here, D represents the grain size; K is a constant typically assumed to be 0.89; λ is the X-ray

wavelength, which has a value of 0.154056 nm for Cu kα targets; β is the FWHM (Full Width at Half Maximum) of the diffraction peak; and θ is the diffraction angle. Furthermore, the mass percentage content of the two phases (ZFO and NNO) in the ZFO/NNO NRs samples was also analysed, with the results indicating a composition of 28.4% and 71.6%, respectively (Figure S1(c)).

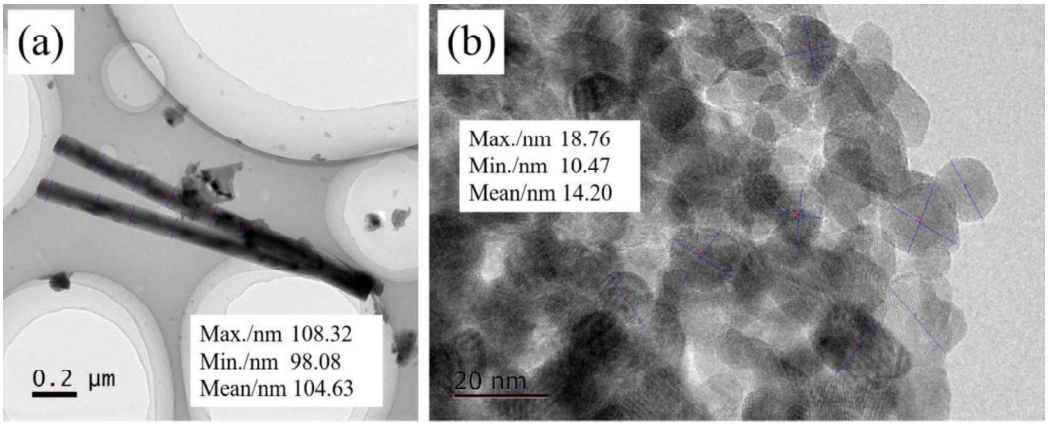

Figure S2. Size measurements of NNO nanorods and ZFO nanoparticles.

The diameter of the NNO nanorod and the size of the ZFO particles were determined utilising the Nano Measurer program (version 1.2.5, developed by Fudan University). Ten points were selected for measurement on the nanorods and nanoparticles, respectively, as illustrated in Figure S2. The diameter of the NNO nanorods is approximately 100 nm, while the size of the ZFO particles is approximately a dozen nanometres.

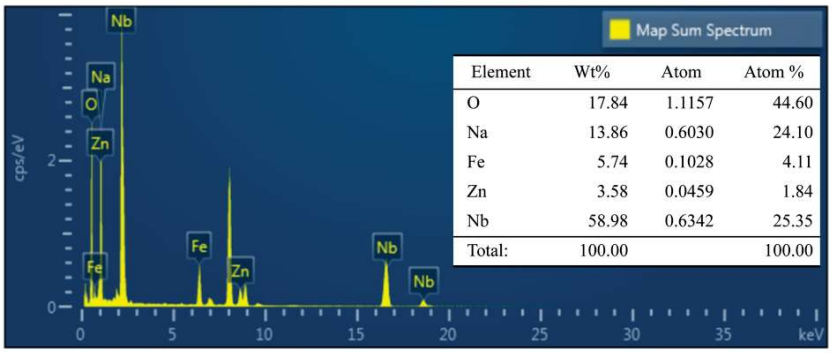

Figure S3. TEM-EDS of ZFO/NNO NR sample.

The mass and atomic fraction percentages of the elements were determined by means of TEM-EDS. The atomic ratio of Fe to Zn is 2.23 (see the inset of Figure S3), which is in close agreement with the stoichiometric ratio of $ZnFe_2O_4$.

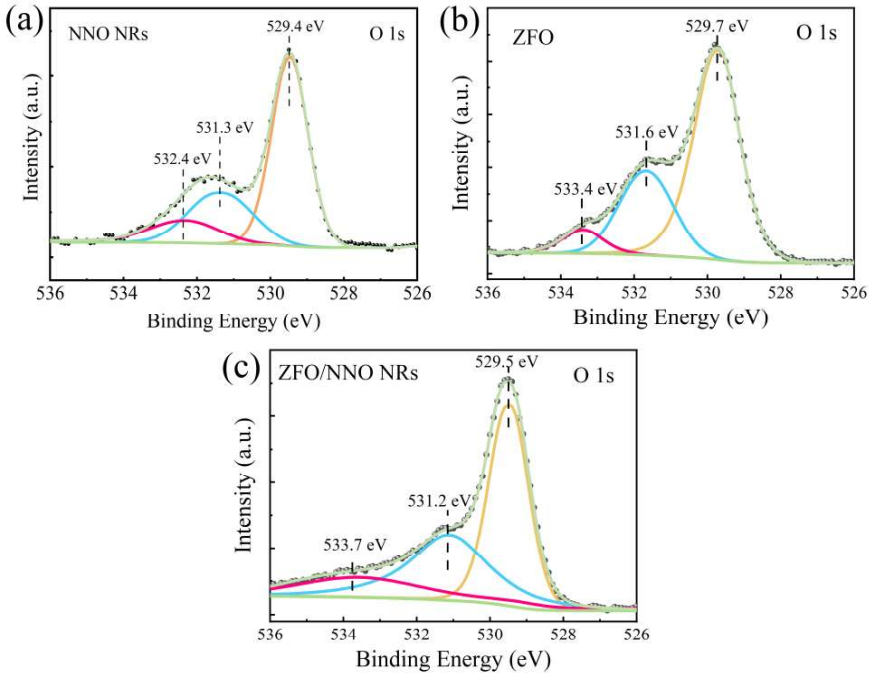

Figure S4. The high-resolution XPS O 1s spectra of (a) the pristine NNO NRs, (b) ZFO and (c) ZFO/NNO NRs heterojunction samples.

The high-resolution XPS O 1s spectra demonstrated that three fitted peaks are attributed to the lattice oxygen in NNO (and ZFO), the surface-adsorbed oxygen in the -OH group, and the oxygen in the chemisorbed H_2O molecule, respectively, with binding energies of approximately

529 eV, 531 eV, and 533 eV [1]. The binding energy at 532.4 eV in NNO is indicative of the presence of weakly adsorbed species and atmospheric contaminants [2].

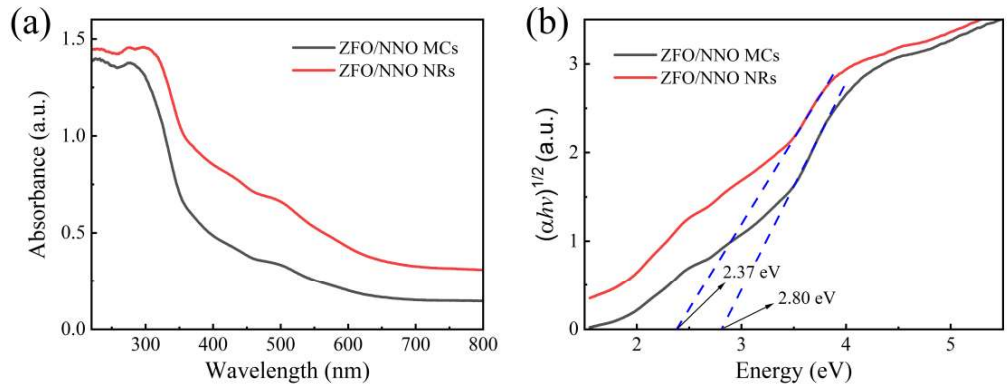

Figure S5. (a) UV–vis absorbance spectra and (b) Tauc plots of ZFO/NNO NR and ZFO/NNO MC.

The UV–vis absorbance spectra and Tauc plots of ZFO/NNO NRs and ZFO/NNO MCs are presented in Figures S5(a) and S5(b), respectively. It can be surmised that the bandgap energies of the ZFO/NNO NR and ZFO/NNO MC are 2.37 and 2.8 eV, respectively.

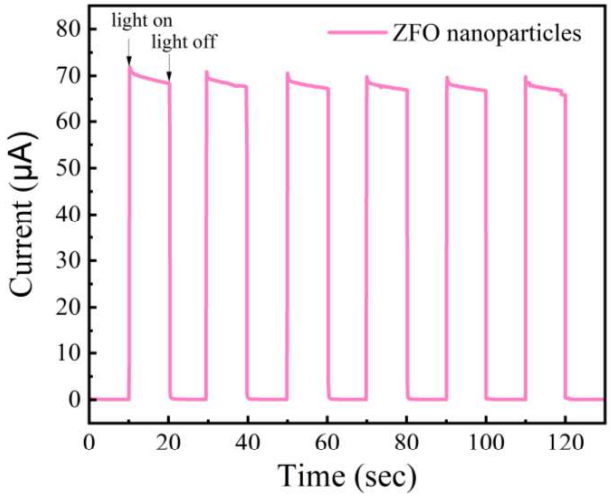

Figure S6. The transient photocurrent response curve of ZFO NPs electrode.

The transient photocurrent response curve of ZFO NPs was measured and presented in Figure

S6. Prior to testing, the ZFO nanoparticles were coated on the FTO surface to fabricate a photoelectrode. The remaining testing conditions were consistent with those described in the experimental section. As can be observed, the photocurrent response was rapid when the light was switched on and off. Following multiple cycles of illumination, the photocurrent intensity demonstrated stability, with a maximum value of approximately 70 μA.

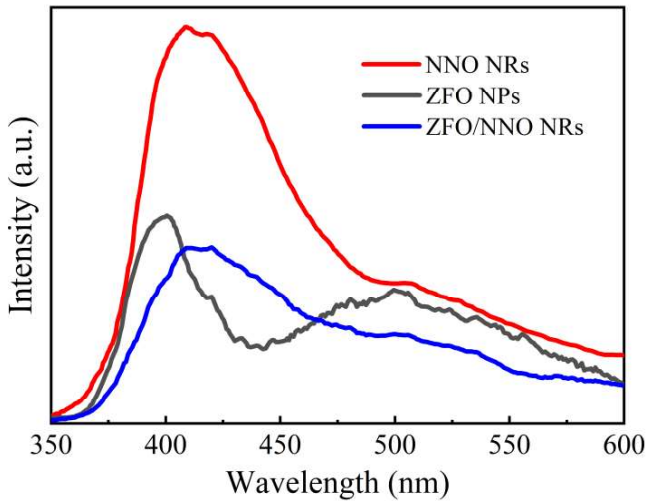

Figure S7. PL spectra of pristine NNO, ZFO and heterojunction samples.

The PL spectra of the pristine NNO, ZFO and heterojunction samples were recorded using an Edinburgh FS5 fluorescence spectrophotometer with an excitation wavelength of 320 nm. As illustrated in Figure S7, the ZFO/NNO heterojunction exhibited a markedly diminished PL intensity in comparison to the pristine ZFO and NNO, which indicates that the ZFO/NNO composite photocatalyst exhibits the highest charge separation ability.

References

[1] Xiaofeng Wang, Jingwen Jiang, Li Yang, Qi An, Qijun Xu, Yongxin Yang, Hong Guo, Enhanced piezoelectric polarization by subtle structure distortion to trigger efficient photocatalytic CO_2RR, Applied Catalysis B: Environmental, 340 (2024) 123177.

[2] Yongpeng Liu, Meng Xia, Liang Yao, Mounir Mensi, Dan Ren, Michael Grätzel, Kevin Sivula, and Néstor Guijarro, Spectroelectrochemical and Chemical Evidence of Surface Passivation at Zinc Ferrite ($ZnFe_2O_4$) Photoanodes for Solar Water Oxidation, Adv. Funct. Mater., 31 (2021) 2010081.